Developmental Biology 432 (2017) 237–247

Contents lists available at ScienceDirect

Developmental Biology

journal homepage: www.elsevier.com/locate/developmentalbiology

Role of maternal *Xenopus syntabulin* in germ plasm aggregation and primordial germ cell specification

Denise Oh, Douglas W. Houston*

The University of Iowa, Department of Biology, 257 BB, Iowa City, IA 52242-1324, USA

ARTICLE INFO

Keywords:
Xenopus
Germ plasm
Primordial germ cells
Germline
Mitochondrial transport

ABSTRACT

The localization and organization of mitochondria- and ribonucleoprotein granule-rich germ plasm is essential for many aspects of germ cell development. In Xenopus, germ plasm is maternally inherited and is required for the specification of primordial germ cells (PGCs). Germ plasm is aggregated into larger patches during egg activation and cleavage and is ultimately translocated perinuclearly during gastrulation. Although microtubule dynamics and a kinesin (Kif4a) have been implicated in Xenopus germ plasm localization, little is known about how germ plasm distribution is regulated. Here, we identify a role for maternal Xenopus Syntabulin in the aggregation of germ plasm following fertilization. We show that depletion of *sybu* mRNA using antisense oligonucleotides injected into oocytes results in defects in the aggregation and perinuclear transport of germ plasm and subsequently in reduced PGC numbers. Using live imaging analysis, we also characterize a novel role for Sybu in the collection of germ plasm in vegetal cleavage furrows by surface contraction waves. Additionally, we show that a localized kinesin-like protein, Kif3b, is also required for germ plasm aggregation and that Sybu functionally interacts with Kif3b and Kif4a in germ plasm aggregation. Overall, these data suggest multiple coordinate roles for kinesins and adaptor proteins in controlling the localization and distribution of a cytoplasmic determinant in early development.

1. Introduction

Cell polarity and intracellular localization in the egg are important for many aspects of normal embryonic development, including overall body patterning and proper germ cell development. The role of a localized “germ plasm” in the formation of the germline has been particularly well studied. Germ plasm was first identified as a histologically distinct region localized within eggs and embryonic germline cells of various organisms and is composed mainly of cytoplasmic aggregates of mitochondria and other organelles, dense ribonucleoprotein germ line granules, and a collection of proteins and RNAs (reviewed in Beams and Kessel, 1974; Houston and King, 2000; Extavour and Akam, 2003; Aguero et al., 2017). The presence of germ plasm and certain localized RNAs is required for germline development in organisms such as *Drosophila*, *Xenopus* and zebrafish. Although maternal germ plasm per se is notably absent from the mammalian egg and early blastocyst (and also from salamander/newt eggs), the differentiating germ cells of these organisms are known to contain a “nuage” substance that is similar in ultrastructure to germ plasm (Eddy, 1975). Nuage also houses a similar set of localized proteins and RNAs and functions during later aspects of germ cell differentiation (Houston and King, 2000; Voronina et al., 2011).

Whereas the overall role of the germ plasm in germ cell biology is well appreciated, the mechanisms controlling its assembly and localization in vertebrates are less well understood. In *Xenopus* eggs, germ plasm is found dispersed in small islands throughout the vegetal cortex (Czołowska, 1969; Whitington and Dixon, 1975). Germ plasm is thought to originate in the mitochondrial cloud/Balbiani body of previtellogenic oocytes, which accumulates germ plasm-specific mRNAs, including *nanos1, dazl,* and *vasa homologs*. The mitochondrial cloud is fragmented during early oogenesis (stage II in *Xenopus*) and its material localizes to the future vegetal pole of the growing oocyte (Kloc and Etkin, 1995; Kloc et al., 1998; Choo et al., 2005). Following oocyte maturation and subsequent fertilization, the germ plasm undergoes additional local clustering and further aggregates into larger masses at the vegetal pole. Aggregation continues during the cleavage stages, mediated in part by surface contraction waves (SCWs) in the egg and blastomeres undergoing mitosis, and is followed by “ingression” of germ plasm along the vegetal cleavage furrows (Ressom and Dixon, 1988; Savage and Danilchik, 1993). At these stages, germ plasm is asymmetrically inherited, resulting in an initial PGC population of about four cells. During gastrulation, the germ plasm transitions from a

* Corresponding author.
E-mail address: douglas-houston@uiowa.edu (D.W. Houston).

http://dx.doi.org/10.1016/j.ydbio.2017.10.006
Received 5 June 2017; Received in revised form 20 September 2017; Accepted 11 October 2017
Available online 14 October 2017

peripheral position to a perinuclear localization and is subsequently inherited symmetrically by daughter cells, presumptively increasing the number of cells specified toward the germline (reviewed in Houston and King, 2000).

Previous inhibitor-based studies in *Xenopus* have indicated that both local and SCW-mediated germ plasm aggregation is microtubule dependent and likely independent of actin microfilaments (Ressom and Dixon, 1988; Savage and Danilchik, 1993). Correspondingly, the germ plasm is enriched in microtubules and depletion of maternal *kif4a* mRNA (*Xklp1*; Robb et al., 1996) inhibited local and SCW-mediated germ plasm aggregation, in the latter case by seemingly inhibiting SCW propagation. Depletion of *kif15* (*Xklp2*) did not affect germ plasm aggregation (Robb et al., 1996), suggesting that different kinesin family members may play discrete roles in germ plasm localization. It is unclear whether Kif4a-mediated germ plasm aggregation is conserved in vertebrates. In zebrafish, germ plasm assembly appears to occur at the cleavage stages and involves a two-stage localization of RNAs to the blastodisc at the animal pole, followed by actin and microtubule mediated mechanisms acting at cleavage furrows (Theusch et al., 2006; Eno and Pelegri, 2016). It is thus likely that the germ plasm assembly process has been modified during evolution of the teleost egg/embryo morphology, and despite the similarity in overall composition and role of the cytoskeleton, the specific mechanisms regulating germ plasm aggregation in either organism are not well understood.

Another conserved cytoplasmic localization event occurring in fertilized eggs is the putative translocation of determinants by microtubule-mediated cortical rotation leading to dorsal axis formation (reviewed in Houston, 2013, 2017). Interestingly, several maternal genes involved in *Xenopus* axis formation exhibit at least partial mRNA localization to the germ plasm in eggs and embryos. These include *trim36*, *dead end homolog 1 (dnd1)* and *plin2*. Importantly, mRNA depletion of maternal stores of these molecules leads to loss of cortical rotation and to defects in dorsal axis formation (Chan et al., 2007; Cuykendall and Houston, 2009; Mei et al., 2013). In zebrafish, two maternal-effect mutants deficient in axis formation have been identified that encode mRNAs localized to the mitochondrial cloud and vegetal cortex of the oocyte and egg (*tokkebi (tkk)/syntabulin (sybu)*, Nojima et al., 2010; *hecate/grip2a*, Ge et al., 2014). Both gene products are potentially involved in microtubule organization and/or trafficking. However, both Sybu and Grip2a protein and RNA fail to accumulate in the aggregating germ plasm following its transport to the forming blastodisc and thus do not localize to embryonic germ plasm. By contrast, in *Xenopus*, *sybu* and *grip2a* do associate with germ plasm in oocytes (Colozza and De Robertis, 2014; Kaneshiro et al., 2007; Tarbashevich et al., 2007) but also remain localized to the germ plasm throughout early embryogenesis. Depletion of Grip2a in fertilized embryos using morpholino antisense oligos in *Xenopus* can result in PGC migration defects (Kirilenko et al., 2008) but a role in axis formation was not specifically tested by depletion of maternal *grip2a* mRNA in oocytes. Maternal depletion of *sybu* by the host-transfer procedure does indeed result in axis deficient embryos (Colozza and De Robertis, 2014) but it remains unclear to what extent Sybu is acting similarly in fish and frogs. Nevertheless, the localization of *sybu* mRNA to the germ plasm in cleavage stage embryos prompted us to examine its roles in the germ plasm.

This work focuses on Sybu, previously characterized as a kinesin motor linker protein involved in the transport of mitochondria, syntaxin-associated vesicles and other cargoes in neuronal axons (Su et al., 2004; Cai et al., 2005, 2007; Frederick and Shaw, 2007). We therefore hypothesized that Sybu would function in linking germ plasm to microtubule motors via mitochondria or other vesicles. Here we show that maternal *sybu* is required for PGC formation in Xenopus, likely by mediating kinesin-dependent aggregation in the early embryo. We also define the roles of additional kinesins in germ plasm aggregation and show that germ plasm aggregation at the vegetal pole is coupled to the surface contraction waves occurring after vegetal cleavage furrow formation.

2. Results

2.1. Syntabulin is associated with germ plasm in Xenopus

In Xenopus and zebrafish, *sybu* is expressed in the mitochondrial cloud/Balbiani body (Bb) of pre-vitellogenic oocytes and in the vegetal

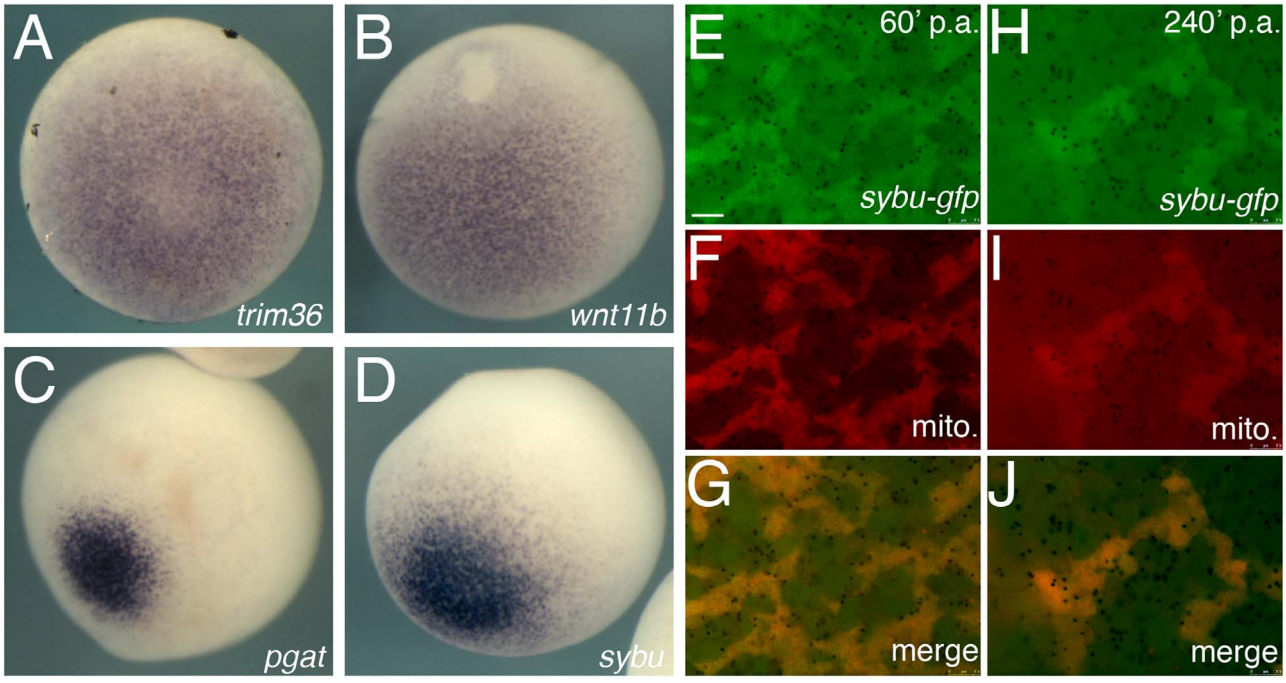

Fig. 1. Germ plasm enrichment of Sybu mRNA and protein in oocytes and early embryos. (A-D) Representative images of whole-mount in situ hybridization on stage VI oocytes comparing expression of (A) *trim36*, (B) *wnt11b*, (C) *pgat* and (D) *sybu*. Vegetal views are shown. (E-J) Localization of Sybu-GFP to germ plasm. (E-G) Overlap of Sybu-GFP with clustered mitochondria (mito., MitoTracker) in pricked eggs 60-min post-activation (p.a.) and at 240-min post-activation (p.a.). Scale bars represent 7.5 μm.

cortex of full-grown oocytes and eggs, congruent with the germ plasm (Colozza and De Robertis, 2014; Nojima et al., 2010). We verified this expression pattern in *Xenopus*, showing as previously reported that *sybu* localizes to the mitochondrial cloud of stage I oocytes and remains with the cloud as it fragments and disperses to the vegetal cortex during oogenesis (Colozza and De Robertis, 2014). In fertilized eggs, *sybu* is maintained in a germ plasm pattern, concentrating at the vegetal apex and at cleavage furrows, and later becoming restricted to a small group of vegetal cells in the gastrula (**Fig. S1**). Because a subset of other vegetally localized RNAs overlapping with the germ plasm have been shown to have roles in axis formation (reviewed in Houston, 2013), it was important to determine whether *sybu* transcript localization mirrored the localization of these other mRNAs. We therefore directly compared the expression of *sybu* to that of other localized RNAs involved in axis formation (*trim36* and *wnt11b*), as well as to that of bona fide germ plasm-localized RNA (*pgat/xpat;* (Hudson and Woodland, 1998)), using oocytes from the same animal under identical conditions.

Sybu localization was more restricted at the vegetal apex, closely resembling the germ plasm-like pattern represented by *pgat* rather than the more intermediate pattern of *wnt11b* and *trim36* (Fig. 1**A-D**). The *sybu* pattern was however consistently broader than *pgat,* which may reflect the localization of *pgat* more exclusively to germinal granules (Kloc et al., 2002). The perdurance of *sybu* in the germ plasm of the dividing embryo in Xenopus differs from zebrafish in this regard; zebrafish *sybu* RNA remains in the vegetal yolk cell during early cleavage and is neither transported to the animal blastoderm cytoplasm nor incorporated into the embryonic germ plasm (Nojima et al., 2010). Also, zebrafish Sybu protein is degraded by 60-min post-fertilization, further suggesting that Sybu protein is not present in the early germ plasm. To determine whether Sybu protein might function in *Xenopus* germ plasm, we injected mRNA encoding a C-terminally-tagged Sybu-GFP fusion protein into oocytes. These were then matured and prick-activated to simulate fertilization and germ plasm aggregation. Sybu-GFP was localized to germ plasm aggregates in the egg, confirmed by co-staining with MitoTracker (Fig. 1**E-J**). And, Sybu-GFP was visible for several hours during germ plasm aggregation, suggesting that at least exogenous protein is not rapidly degraded after fertilization. Overall, these data show that *Xenopus* Sybu is localized to aggregating germ plasm in the embryo, although lack of specific antibodies precluded analysis of the endogenous protein localization.

2.2. Depletion of maternal syntabulin results in reduced primordial germ cell formation

To determine the extent that the germ plasm localization of maternal Sybu correlated with a role in normal germ cell development, we used an antisense oligo-mediated maternal mRNA depletion strategy (reviewed in Hulstrand et al., 2010). Although Colozza and De Robertis (2014) identified a role for Sybu in dorsal axis formation, our own oligo design identified several oligos that appeared to substantially deplete *sybu* RNA (Fig. 2**A**) although none of these resulted in ventralization (see below). X. laevis is an ancient allopolyploid with a genome comprising two “subgenomes,” L and S (corresponding to Long and Short homeologous chromosomes) derived from the hybridization of two ancestral species (Session et al., 2016). In many cases, transcripts are expressed from both homeologs and we suspected a potential incomplete targeting of one homeolog. *Sybu* is retained in both subgenomes, in contrast to typical core germ granule genes, which are preferentially retained within the L subgenome (Session et al., 2016). We therefore determined the extent of knockdown of *sybu.L* and *sybu.S* homeologs.

A comparison of candidate oligo sequences showed that our most effective oligo, *as234*, was 100% identical to *sybu.S* (the homeolog on chromosome (chr) 6 S) but had one mismatch in the central region to *sybu.L* (chr6L). In contrast, the oligo identified by Colozza and De Robertis as6) (2014) was 100% identical to both L and S homeologs. Specific qRT-PCR primers and hydrolysis probes were used to detect the *sybu.S* and *sybu.L* homeologs in oligo-injected and control oocytes. Whereas both oligos were effective in reducing *sybu.S* to below ~ 12% of control levels, *as234* was less effective at causing depletion of *sybu.L*, which remained at about 25% of control levels (Fig. 2**B**). However, overall *sybu* levels, as assessed by primers that amplify both homeologs, were nonetheless substantially depleted by oligo *as234*.

Because our pilot studies had suggested that embryos depleted of *sybu* using oligo *as234* were not phenotypically ventralized, and because of *sybu*'s germ plasm localization, we took the opportunity to use this oligo to investigate whether Sybu might have an additional role in primordial germ cell (PGC) formation. This process cannot be effectively monitored in ventralized embryos owing to the involvement of dorsally derived structures. Embryos lacking maternal *sybu* were obtained by injecting cultured oocytes with oligo *as234* and fertilizing these following host transfer into egg laying females. At doses of both 3.0 ng and 6.0 ng we recovered numerous fertilized eggs and these developed normally through gastrulation and formed normal swimming tadpoles (Fig. 2**C**). We assessed the extent of primordial germ cell development in *sybu*-depleted embryos by examining *pgat* expression in tailbud stage embryos, which identifies migrating PGCs at this stage (Hudson and Woodland, 1998). Control embryos derived from uninjected oocytes showed numerous *pgat*-expressing primordial germ cells in the endoderm, likely in the process of migrating to the future dorsal mesentery (Fig. 3**A**). In *sybu*-depleted embryos, these migrating PGCs were either absent or severely reduced in number (Fig. 3**B**). To demonstrate the specificity of this effect on PGCs, we reintroduced in

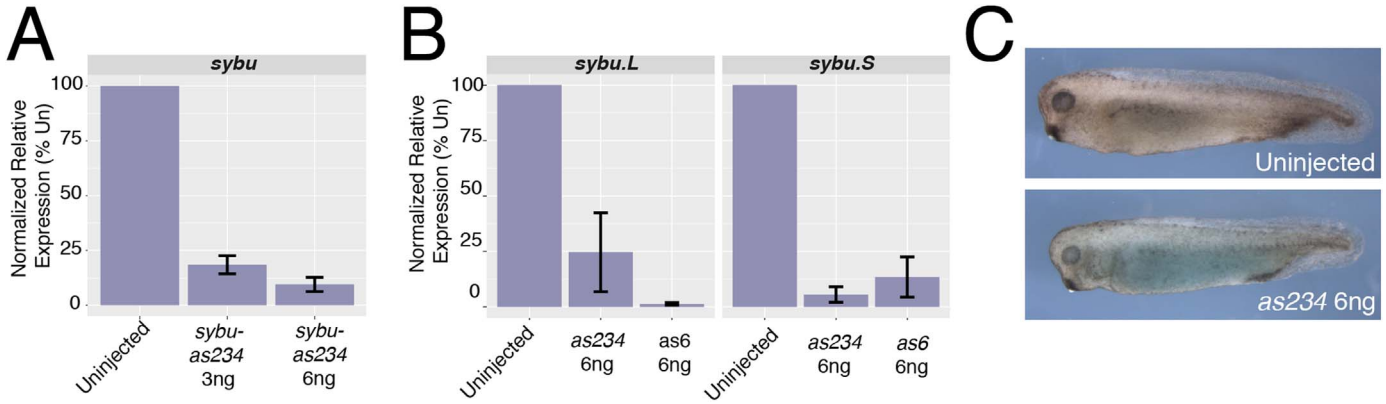

Fig. 2. Antisense oligo-mediated depletion of *sybu*. (A) Real-time RT-PCR analysis of total *sybu* levels following injection of *as234*. (B) Differential depletion of *sybu* homeologs by *as234* and *as6* oligos. (C) Representative embryos obtained from host-transfer experiments using Uninjected control oocytes (upper panel) or *sybu*-depleted oocytes (lower panel). In (A-B), bars represent the average of two experiments; errors bars represent standard errors.

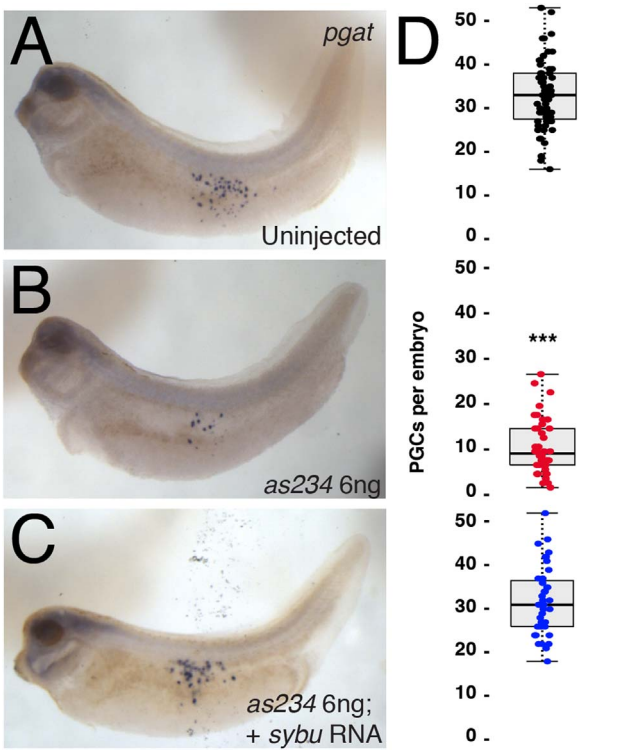

Fig. 3. Reduction of PGCs in *sybu*-depleted embryos. (A-C) Whole-mount in situ hybridization for *pgat* mRNA. (A) control uninjected embryo, (B) *sybu*-depleted embryo, (C) depleted embryo rescued with injected *sybu* mRNA (5 pg). (D) Scatter plots of PGC numbers in experimental groups corresponding to the adjacent panel. Dots represent individual in which PGCs were counted (sum of three separate host-transfer experiments); dark line represents the median; shaded areas correspond to the limits of the first and third quartiles (25th/75th percentiles) and whiskers (dotted line) extends out to 1.5x the interquartile range. $P < 0.001$ by Kruskal-Wallis test; *** = $P < 1.0e\text{-}11$ by Dunn's post hoc test w/ 2-sided Bonferroni adjustment.

vitro-transcribed *sybu* mRNA into depleted oocytes. PGC numbers were similar to control numbers in these rescued embryos, and the extent of migration also resembled the normal cases (Fig. 3**C**). These data suggested that in addition to possible functions in axis formation, in Xenopus Sybu likely has roles in the germ plasm to control either PGC specification and/or migration.

2.3. Syntabulin is required for proper germ plasm aggregation and localization in the embryo

We next wished to more precisely determine at which stage germline development becomes disrupted in the absence of Sybu. Maternal *sybu*-depleted embryos were examined over a time course of early germ plasm aggregation and relocalization. Germ plasm organization was initially assessed by staining for *pgat* RNA. In early cleavage-stage embryos derived from control uninjected oocytes, *pgat* RNA accumulates in aggregated germ plasm along vegetal cleavage furrows. In *sybu*-depleted embryos however, we saw reduced and uneven aggregation of germ plasm islands. These aggregates were smaller and dispersed away from vegetal cleavage furrows, in contrast to the rather compact pattern of germ plasm observed in controls (Fig. 4**A-C**). This pattern of mislocalization was also evident at the morula stage (32-cell, Fig. 4**A'-C'**) and into the gastrula stages, where germ plasm remained scattered in smaller islands throughout vegetal cells (not shown). Depletion using either oligo *as234* or *as6*, which target different regions of *sybu* mRNA, showed similar germ plasm aggregation defects during cleavage stages. And, as with the PGC migration phenotype, reintroduction of *sybu* transcripts (5 pg per embryo) could rescue the effects of both oligos and restore normal aggregation (Fig. 4**D, D'**), thus confirming the specificity of the effects of oligo injection.

Relocalization of germ plasm from the cortex to the perinuclear region is an important hallmark of PGC specification. We therefore next sought to determine whether early germ plasm aggregation defects correlated with defects in perinuclear localization. Gastrula stage germ plasm is internal and not easily examined using in situ hybridization. We therefore briefly stained early embryos with the lipophilic dye DiOC6(3) to label the mitochondria-rich germ plasm (Savage and Danilchik, 1993; Venkatarama et al., 2010) and then dissected the vegetal mass from gastrula-stage embryos. This tissue was dissociated and cells examined by epifluorescence microscopy to identify germ plasm-containing cells. These presumptive PGCs could be readily identified and typically showed a bright cluster of germ plasm adjacent to the nucleus (Fig. 5). DiOC6(3)-labelled cells were more difficult to find in *sybu*-depleted embryos, but in ten cases where the labeling was robust, the germ plasm was invariably located near the cortex or dispersed between the cortex and nucleus (Figs. 5**B,** 5**B'**). Overall, these data suggest that Sybu is necessary for germ plasm aggregation following fertilization, clustering a critical mass of germ plasm at the vegetal pole, and may also be required directly and/or indirectly for influencing the subsequent perinuclear accumulation of germ plasm for

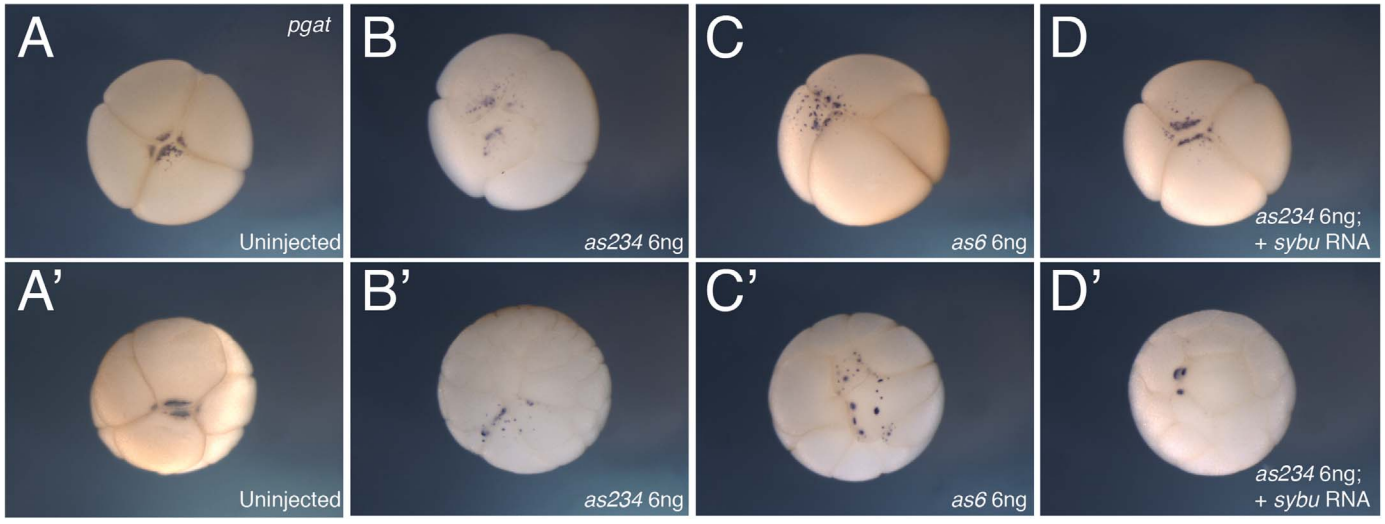

Fig. 4. Abnormal germ plasm aggregation in *sybu*-depleted embryos. (A-D) Representative embryos at the 4-cell stage, probed for *pgat* to identify germ plasm, vegetal views. (A) uninjected control embryo, (B) *sybu*-depleted embryo, using *as234*, (C) *sybu*-depleted embryo using *as6*, (D) *sybu*-depleted embryo (as234) rescued by injection of *sybu* mRNA. (A'-D') Representative embryos similarly analyzed at the 32-cell stage.

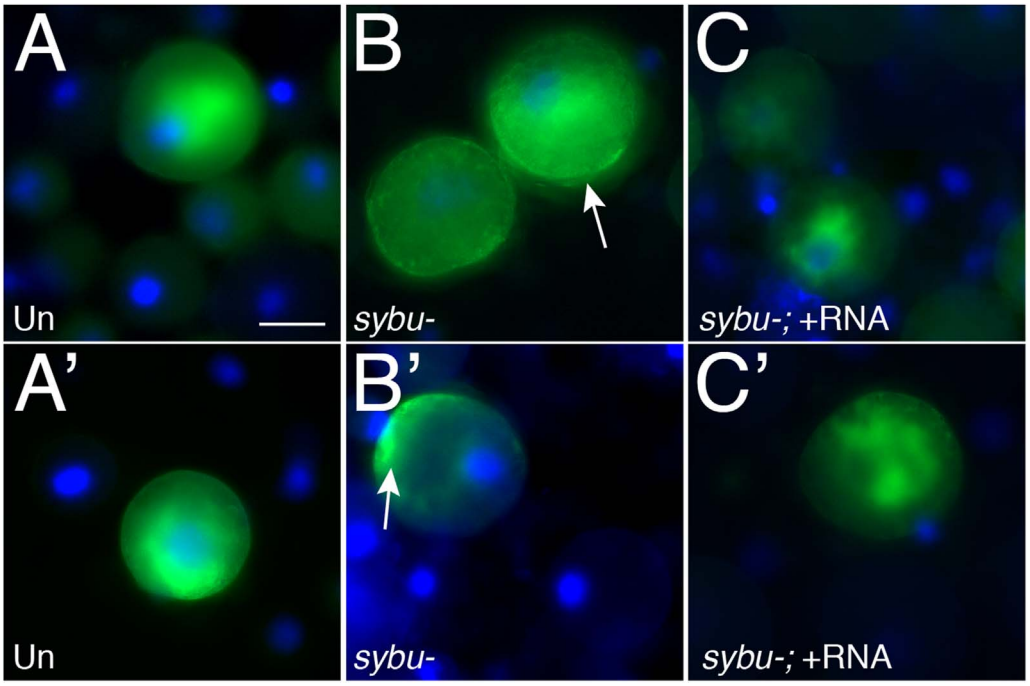

Fig. 5. Failure of peri-nuclear germ plasm localization in *sybu*-depleted embryos. (A-C') DiOC6(3) staining in isolated blastomeres (Green; DAPI in blue). Embryos were stained at the 4-cell stage and dissociated at the early gastrula stage. (A, A') control uninjected isolated vegetal blastomeres, (B, B') *sybu*-depleted blastomeres, (C, C') blastomeres rescued by *sybu*-mRNA injection. arrows = cortical mitochondrial/germ plasm enrichment; scale bar = 30 μm.

proper PGC specification.

2.4. Second SCW-driven germ plasm localization to vegetal pole cleavage furrows requires Sybu

Because our results indicated a defect in overall germ plasm aggregation in *sybu*-depleted embryos, we next sought to determine which aspects of this process might require Sybu function. Insofar as germ plasm aggregation has been investigated at the cellular and molecular level in Xenopus, aggregation requires microtubules (although not microfilaments) and the motor protein Kif4a, for generating and/or propagating SCWs that drive germ plasm clusters toward the vegetal cleavage furrows (Quaas and Wylie, 2002; Savage and Danilchik, 1993).

To further address this issue, we performed live imaging of control and *sybu*-depleted oocytes fertilized following host-transfer (Figs. 6 and 7**; Supplementary Videos 1 and 2**). Fertilizing eggs in small batches, we imaged eggs at low magnification using time-lapse epifluorescence microscopy (frame rate = 20 s), filming at least three eggs per sample per experiment over three experiments using eggs/oocytes from different donor females. Germ plasm was visualized by brief labeling with the lipophilic dye DiOC6(3) to preferentially stain mitochondria enriched in germ plasm (Ressom and Dixon, 1988; Savage and Danilchik, 1993; Quaas and Wylie, 2002). Movies were started at roughly eighty minutes after fertilization, to capture the end of cortical rotation (as an internal control for normal development), and then continued for ninety additional minutes (170 min post-fertilization total) to visualize the aggregation process.

Supplementary material related to this article can be found online at doi:10.1016/j.ydbio.2017.10.006.

In control eggs (n = 10/10), DiOC6(3)-labelled germ plasm is seen translocating with the vegetal yolk mass during cortical rotation until the appearance of the first mitotic SCWs, at which point cortical rotation ceases. In agreement with previous studies, germ plasm did not substantially aggregate during cortical rotation (Savage and Danilchik, 1993). Aggregate size did not visibly increase following the passage of the first SCWs, suggesting little aggregation, whereas a greater amount of aggregation was seen in response to cytoplasmic perturbations created by the first cleavage furrow (Fig. 6**A, Supplementary Video 1**). Subsequently, prior to second cleavage, germ plasm clusters grew slightly larger following the passage of the SCW of the second mitosis (~15 min pre-furrow). At the end of this set of SCWs, or the final continuation of it, a subset of germ plasm clusters became visible at the egg surface and were then rapidly swept toward the vegetal pole, accumulating in a large patch along the furrow. A similar process was repeated after the formation second cleavage furrow, resulting in the typical four "island" pattern typical of germ plasm. The events in these movies were analyzed using kymographs, in which SCWs were evident as lateral waves (Fig. 6**B**). The collection along the furrow at the end of the second SCW appears as an interruption in the wave pattern and as a hazy area in the kymograph, as the particles become grouped in larger areas (bottom, Fig. 6**B**).

In *sybu*-depleted embryos, DiOC6(3)-labelled germ plasm translocated normally during the period of cortical rotation (Fig. 6**C, Supplementary Video 2**), however there was no noticeable increase in aggregation following first cleavage. Further, the formation of dispersed particles and their collection along the vegetal cleavage furrows was much diminished or absent (n = 9/10) and kymographs did not show evidence of perturbation by SCWs or of furrow aggregation (Fig. 6**D**). To validate the specificity of this aspect of the *sybu* depletion phenotype, we also made movies of rescued embryos (**Supplementary Video 3**) and found that the appearance of rapid translocation vegetally was restored (n = 3/3).

Supplementary material related to this article can be found online at doi:10.1016/j.ydbio.2017.10.006.

To better quantify the effect of *sybu* depletion on germ plasm aggregates, we estimated DiOC6(3)-labelled aggregate size in frames at 10-min intervals from three movies of control and *sybu*-depleted eggs. We consider these only estimated sizes owing to loss of information through imaging of a round egg and because of the thresholding involved in image processing. Frames were extracted from movies and exported using Fiji/ImageJ, followed by thresholding and measurement using a custom Matlab script. Examples of the processed images and the average germ plasm aggregate area in control and experimental

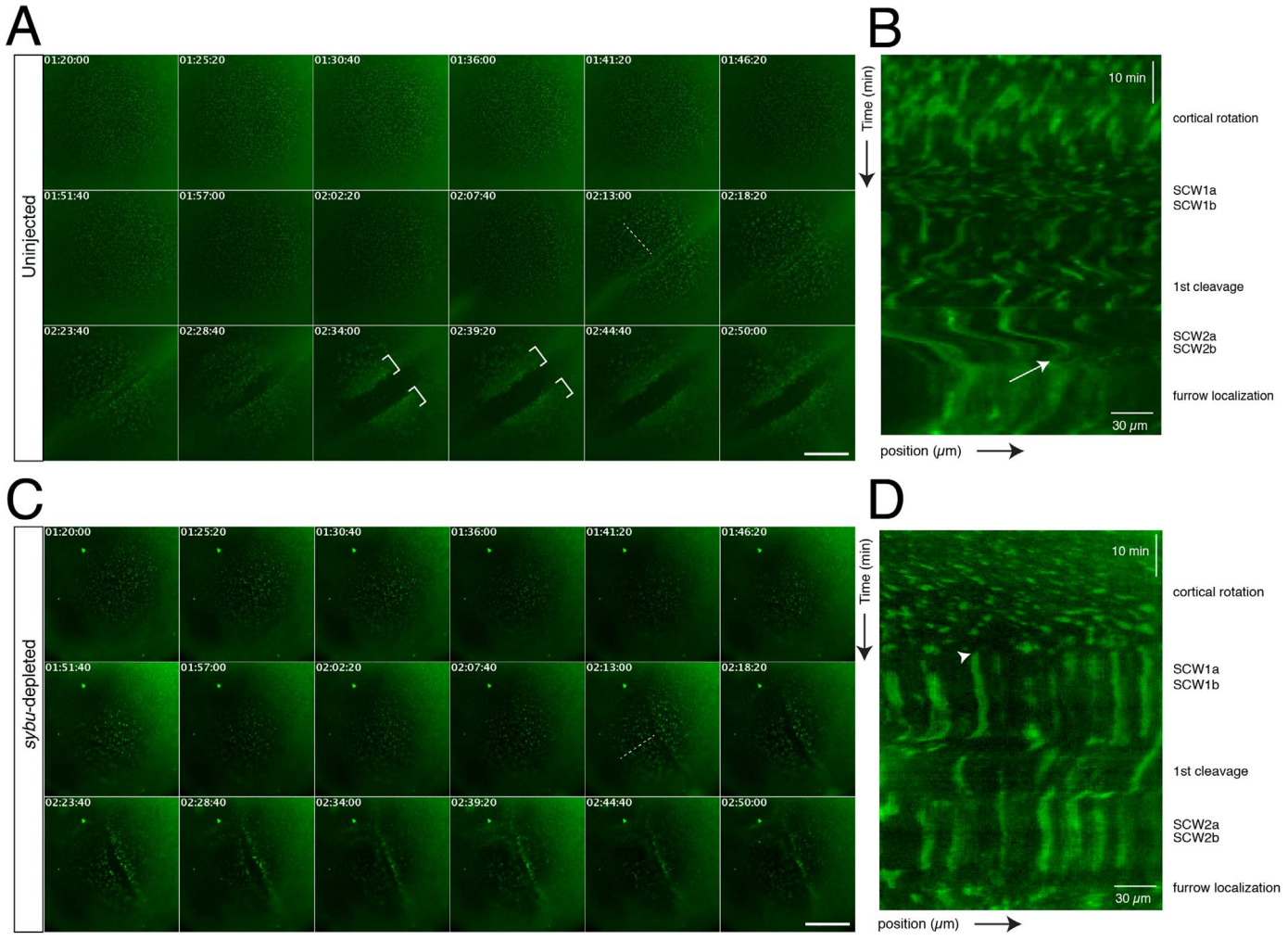

Fig. 6. Time lapse imaging of germ plasm aggregation during early development in host-transfer fertilized eggs. (A) Representative time-lapse imaging of a zygote obtained by the host-transfer procedure, stained with DiOC6(3). Panels in (A) show selected frames at ~5-min intervals from Supplementary Video 1 (170 min time-lapse, frame rate = 20 s). In (A, C), elapsed time from in vitro fertilization is shown at the top of each frame (in h:min:sec); dotted lines indicate the lines used for kymograph profiles; brackets indicate areas of clustered germ plasm; scale bars = 85 μm. (B) Representative kymograph analysis of an uninjected control embryo. The approximate timing of post-fertilization events is shown on the right. The white arrow indicates the beginning of aggregation into larger areas at the tail end of SCW2a/b. The position arrow indicates distance from the vegetal pole (bottom left corner). (C) Representative time-lapse imaging of a *sybu*-depleted zygote obtained by the host-transfer procedure, stained with DiOC6(3) (labels as in A). Panels show selected frames at ~5-min intervals from Supplementary Video 2. (D) Representative kymograph analysis of a *sybu*-depleted embryo. Germ plasm is not disturbed by SCWs (arrowhead) and fails to form large continuous aggregates at the cleavage furrows.

eggs are shown in Fig. 7. As evident from the movies, these measurements show little change in aggregate size during cortical rotation and in response to the first SCWs (80–90 min), as well as during the period up to the first cleavage furrow formation (140', Fig. 7**E**), at which time there is a slight but significant increase. Consistent with the lack of aggregation in the absence of *sybu*, the average germ plasm aggregate size remained unchanged during the period of analysis (Fig. 7**F**).

Taken together, these observations highlight several aspects of Sybu-dependent germ plasm aggregation: 1) as reported, little to no germ plasm aggregation happens during cortical rotation (Quaas and Wylie, 2002; Savage and Danilchik, 1993); 2) SCWs in general do not drive aggregation at the furrows – the 1st SCWs promote some local aggregation whereas the 2nd (and subsequent) SCWs promote large-scale collection of germ plasm at the cleavage furrows; 3) noticeable aggregation occurs after the passage of cleavage furrows, and 4) only a subset of clusters and/or germ plasm within a cluster become enriched at the furrow.

2.5. Sybu functionally interacts with multiple Kinesin-related proteins in germ plasm aggregation

In the context of both neuronal transport and early zebrafish development, Sybu has been suggested to serve as a linker for Kif5b/KinesinI (Su et al., 2004; Nojima et al., 2010). The extent that Sybu might interact with different kinesins to mediate germ plasm aggregation in the Xenopus egg is unknown. Kif4a has been implicated, likely acting through the generation and or maintenance of SCWs, although its protein is also enriched in germ plasm (Robb et al., 1996; Quaas and Wylie, 2002). Prior maternal depletion experiments ruled out a role for Kif15/Xklp2 (Robb et al., 1996). Kif5b has not been explicitly tested in Xenopus germ plasm aggregation, although inhibitory antibody studies suggest it is dispensable for other microtubule-dependent events including cortical rotation and melanosome dispersal. Interestingly, we also noted from the literature that *kif3b* mRNA and protein is localized to the germ plasm in Xenopus oocytes (Betley et al., 2004), resembling *sybu*.

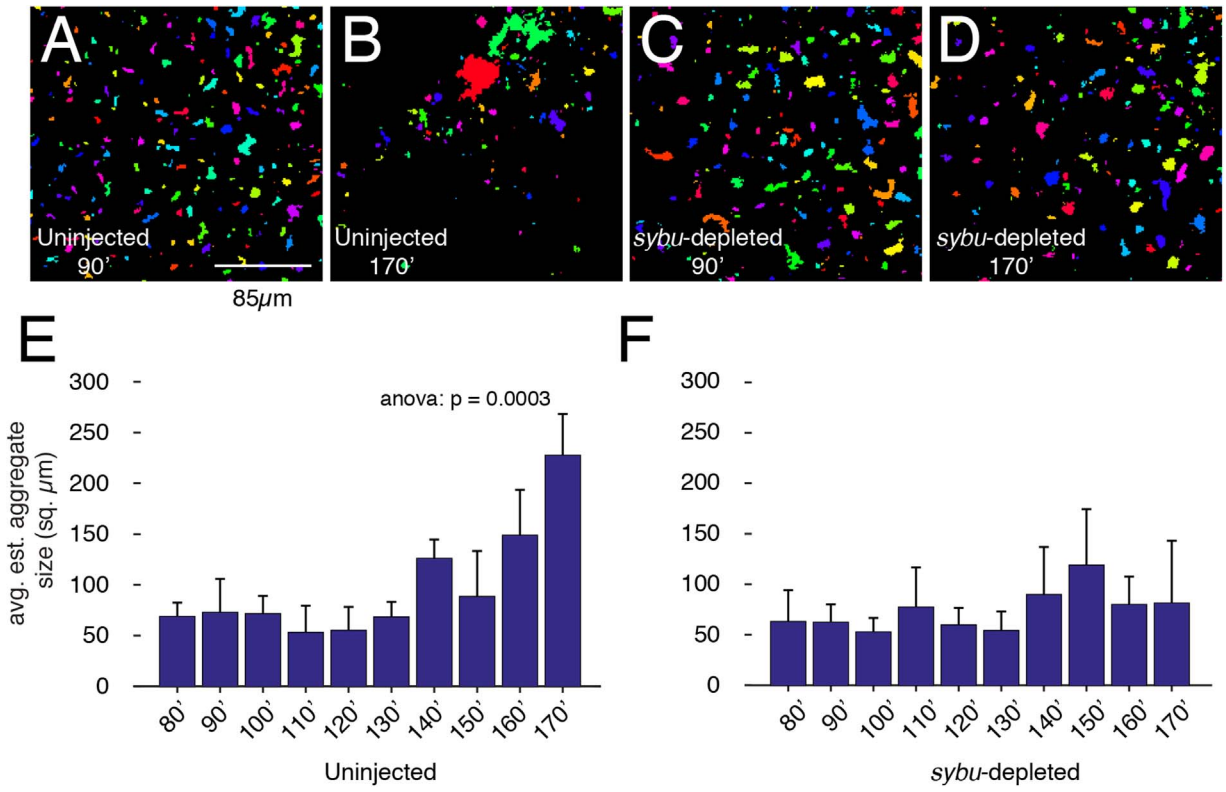

Fig. 7. Quantification of germ plasm aggregation in early development. (A-D) Representative images from time-lapse videos (Videos 1, 2) from uninjected and *sybu*-depleted embryos, showing frames analyzed at ~90 min (A, C) and ~170 min (B, D) after fertilization. Vegetal views. Thresholded areas were randomly pseudocolored to verify that they could be distinguished and measured as separate clusters. (E-F) Graphs showing mean aggregate size at the indicated time points; error bars indicate standard errors. N = 3 host-transferred eggs; > 100 germ plasm aggregates (three experiments). The p-value from one-way ANOVA is indicated at the top. Scale bar in A-D = 85 μm.

To begin to determine whether Sybu might act with these kinesins in germ plasm aggregation, we determined the extent of functional interaction between Sybu and kinesins Kif4a and Kif3b. We designed antisense oligos against *kif3b* and used a published oligo sequence against *kif4a* to deplete these mRNAs from oocytes (Fig. S2**A**). These were injected into oocytes and germ plasm aggregation was assessed by prick-activating these after progesterone-induced maturation (Fig. 8**A**). Pricking mimics fertilization and these oocytes will undergo normal cellular events like cortical rotation and germ plasm aggregation but not cleavage. For analyzing and comparing larger numbers of samples, this experimental design is often preferable to using host-transferred eggs. Consistent with our results presented above and with published reports (Robb et al., 1996; Quaas and Wylie, 2002), we found that germ plasm aggregation (here labelled using Mitotracker) was specifically reduced in *sybu*- and *kif4a*-depleted eggs 3–4 h after prick activation. (Fig. 8**B-F**). Germ plasm aggregation was also significantly reduced to a similar extent in *kif3b*-depleted eggs (Fig. 8**F**), with all eggs examined lacking large aggregates ($p < 0.001$; n = 20). Furthermore, germ plasm aggregation was reduced in *kif3b*-depleted eggs fertilized by host transfer and analyzed by live imaging (**Supplementary Video 3,** Fig. S3, n = 5/5). Although these embryos cleaved normally, all but a few were arrested in gastrulation and did not survive. This precluded an analysis of germ cell formation but suggested a role for maternally-supplied Kif3b in possibly establishing cell polarity during convergent extension gastrulation movements, as hypothesized by Shindo et al. (2008).

To provide insight into whether Sybu might be working with these kinesins to mediate germ plasm aggregation, we performed functional interaction studies using combinations of sub-effective oligo doses to partially deplete each component. Whereas the individual lower oligo-injected groups showed normal aggregation, the combinations of low-dose *sybu* oligos with either low-dose *kif4a* or *kif3b* oligos reduced germ plasm aggregation to a significant extent (Fig. 8**G;** $p < 0.001$; n = 20). Taken together, these data demonstrate that Sybu likely mediates germ plasm aggregation by interacting with at least two kinesin motors, Kif4a and Kif3b.

3. Discussion

The role of cytoplasmic inheritance of a localized “germ plasm” during the specification of the germline has long-been appreciated but the mechanisms that assemble and localize the germ plasm (and the degree that these mechanisms are conserved) are little understood. Here we show a role for maternal *syntabulin*, which is localized to the germ plasm, in the aggregation of germ plasm during the cleavage stages of early Xenopus development and subsequent specification of PGCs. Interestingly, we noted that normal germ plasm aggregation likely involves localization towards cleavage furrows by surface contraction waves in the dividing egg. Syntabulin has been implicated as a protein linking kinesins to various cargo, including mitochondria, Syntaxin-containing vesicles and (in Xenopus and zebrafish) putative dorsal determinants (reviewed in Hirokawa et al., 2009; Houston, 2017). Our work shows that Sybu functionally interacts with a wider range of kinesins and has adopted an additional role in germ plasm aggregation in Xenopus.

We used antisense-based loss-of-function experiments to elucidate the role of maternal *sybu* in Xenopus. Prior studies have shown embryos derived from *tokkaebi* mutant female zebrafish are variably ventralized in a manner sensitive to genetic background (Nojima et al., 2010) and Xenopus embryos derived from oocytes injected with *sybu* antisense oligos are also ventralized to some extent (Colozza and De Robertis, 2014). Interestingly, we designed several antisense oligos that substantially depleted maternal *sybu* mRNA in Xenopus oocytes but did not generate ventralized embryos. Although extensive transcrip-

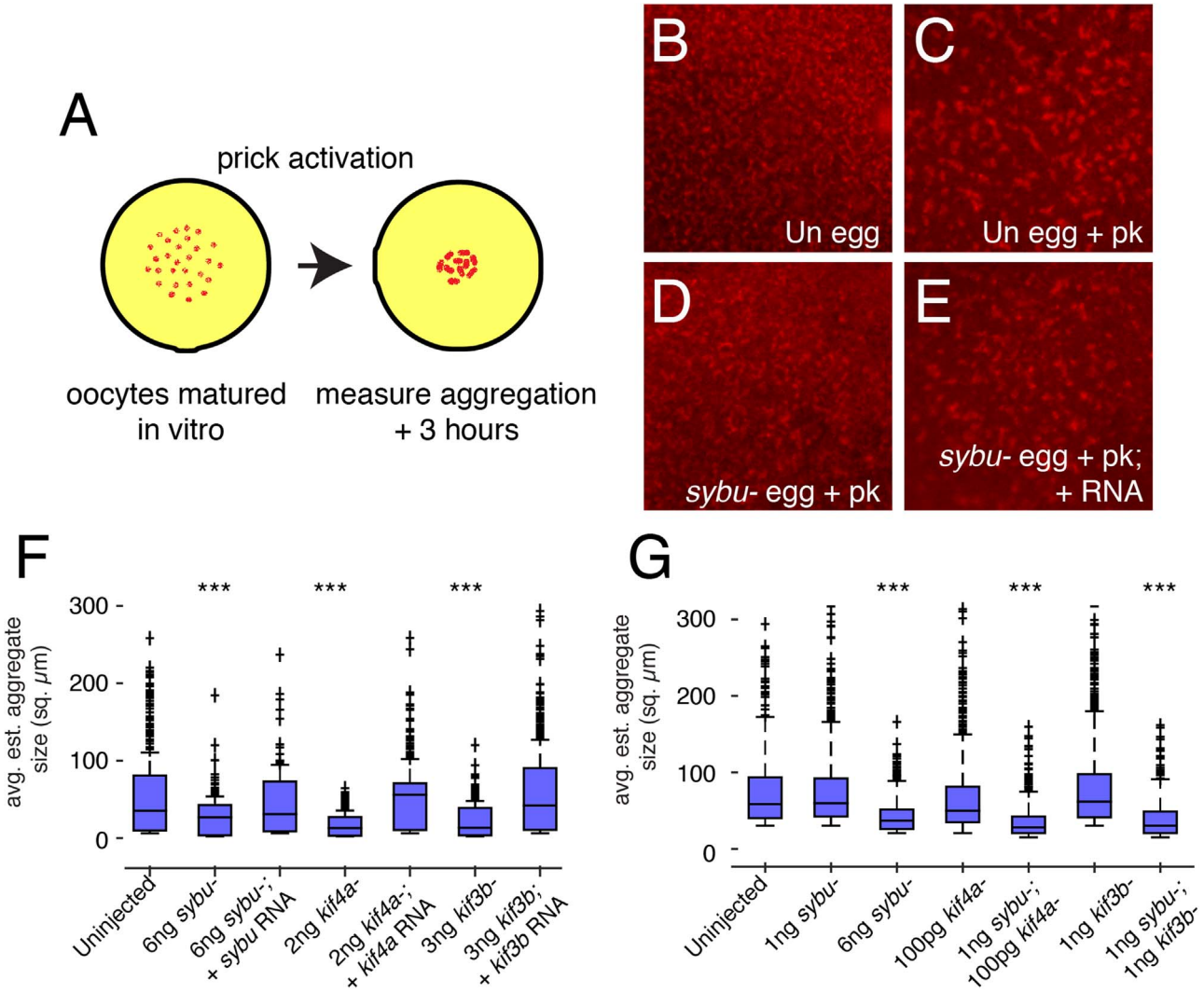

Fig. 8. Functional interaction of Sybu with kinesins Kif3b and Kif4a in germ plasm aggregation. (A) Model of the experimental design. Oocytes are stained with MitoTracker and imaged following prick-activation. (B-E) Representative images control eggs before and after aggregation (B, Uninjected (Un) egg; C, Un egg + prick activation (pk)) and of *sybu*-depleted and rescued prick-activated eggs (D, *sybu*- egg +pk; E, *sybu*- egg +pk + RNA). (F-G) Average germ plasm aggregate size in depleted and rescued groups (F) and in different combinations of sub-effective doses of oligos (G). The dark bar in each box indicates the median size per group, lower and upper edges of the colored boxes indicate 25th and 75th percentiles respectively, whiskers represent maximum and minimum adjacent values. Outliers (> 1.5x interquartile range) are indicated by crosses (+). N = 20 oocytes, > 500 total islands. ***$P <$ 0.001 by Kruskal-Wallis test/Dunn's post-hoc.

tome and genome sequence data has been available for the diploid Xenopus tropicalis (Hellsten et al., 2010) for some time, this has only recently become accessible for Xenopus laevis (James-Zorn et al., 2015; Karpinka et al., 2015; Session et al., 2016). Upon retrospective inspection of our oligo sequences, we found our most effective oligo (*as234*) contained a one base mismatch with one of the homeologs (*sybu.L*) and depleted this homeolog to a lesser extent. Therefore, it may either not deplete enough of the *sybu.L* homeolog mRNA or of overall *sybu* to elicit ventralization, whereas the role of Sybu in the germ plasm may be more sensitive to depletion. Regardless, embryos derived from oocytes injected with this oligo develop reproducible and rescuable defects in primordial germ cell formation and germ plasm aggregation.

It is unclear to what extent these homeologs have become sub-functionalized in Xenopus. The *sybu.S*-homeolog is expressed at twice the level of *sybu.L* (RNAseq data from Session et al., 2016 accessed on Xenbase; (James-Zorn et al., 2015; Karpinka et al., 2015; Session et al., 2016)). And, the rescue construct used by ourselves and Colozza and De Robertis (2014) encodes the S-homeolog. There is little amino acid difference between the two forms that might account for the different functions. It is thus unclear whether a suboptimal depletion of a minority species (the L-homeolog) would be responsible for the lack of ventralization in our hands. Similar to the zebrafish, there may be strain-specific requirements for Sybu in axis formation in different outbred populations Xenopus. It would be useful to repeat some of these experiments in several of the inbred Xenopus strains that have recently become available. Regardless of the role of Sybu in axis formation, our data show that Sybu also functions in germ plasm aggregation, resulting in loss of PGCs by the tailbud stage. We show this with both the *as234* oligo and *as6* oligo (Colozza and De Robertis, 2014), and the effects on aggregation can be rescued by injection of *sybu*.

We see several defects in PGC specification in embryos depleted of maternal *sybu*. First, germ plasm fails to aggregate into large “islands” at the vegetal pole, and during gastrulation, the germ plasm fails to become perinuclear. Therefore, one proximal cause of fewer PGCs in *sybu*-depleted embryos is likely to be this lack of perinuclear recruitment. Perinuclear localization has long been thought to be indicative of germ plasm “activity” (e.g., Blackler, 1958) but its mechanistic function is unclear. Our data do not distinguish between a direct role for maternally supplied Sybu in transporting germ plasm perinuclearly or whether this is a consequence of earlier aggregation defects or lack of a

critical mass of germ plasm. In either case, presumptive PGCs receiving *sybu*-depleted germ plasm are likely not specified properly and do not initiate migration.

In examining the dynamics of germ plasm aggregation, we noted a correlation of cleavage furrow formation and the accumulation of germ plasm into large vegetal islands. Current models of germ plasm aggregation suggest this occurs through local Brownian aggregation, augmented by surface contraction waves (Quaas and Wylie, 2002). Our observations suggest several refinements to this model. First, we find that not all SCWs are involved in aggregation. We saw little aggregation in response to the first set of SCWs preceding first cleavage. These occur at the end of cortical rotation, during which we and others have found that no aggregation occurs. Also, in our hands local aggregation is enhanced by cleavage furrow formation, after which individual clusters appear larger. Importantly we show that end of the second set of SCWs, after first cleavage and prior to 2nd cleavage, germ plasm is robustly driven towards the vegetal cleavage furrow. Similar processes occur after the 2nd division, resulting in the typical "four-island" appearance of germ plasm.

These results are interesting because they suggest that aggregation occurs by a more dynamic process than previously thought. Many germ plasm clusters remain unaggregated after SCW passage, indicating that this is not simply a physical response to SCWs. This aspect could be indicative of an underlying cytoskeletal regulation, likely involving transport on microtubules by Kinesin-Sybu and other motor complexes. Organized microtubules are present near the cleavage furrows, termed the furrow microtubule array (FMA; Danilchik et al., 2003) and it is possible these microtubules mediate germ plasm transport.

Our work identifies several kinesins likely to mediate Sybu-mediated germ plasm transport. Using functional interaction in RNA depletion studies, this work suggests that germ plasm aggregation is mediated by Kif4a and Kif3b interacting with Sybu. Kif4a was previously shown to be required for germ plasm aggregation but its role remains unclear. Kif4a depleted embryos fail to undergo normal mitosis and thus do not generate SCWs, secondarily impacting germ plasm aggregation. Kif4a protein is also enriched in germ plasm and local aggregation is affected (Robb et al., 1996), suggesting a dual role. Because SCWs are normal in Sybu-depleted embryos, and Sybu is also enriched in the germ plasm, we infer that Sybu could mediate the local aggregation function of Kif4a. Kif4a has been implicated in vesicle transport as well as spindle regulation, although mitochondria have not been specifically examined (reviewed in Hirokawa et al., 2009). Human *KIF4A* has been implicated in synaptic dysregulation, which likely involves presynaptic mitochondrial localization (Willemsen et al., 2014), suggesting a possible role for Sybu-Kif4a complexes in this process.

Prior work also indicated localization of Kif3b to the germ plasm and implicated its function in RNA localization and/or germ plasm localization during oogenesis (Betley et al., 2004; Messitt et al., 2008). Our work shows that depletion of Kif3b generally mimics Sybu depletion with regard to germ plasm aggregation. Thus, Kif3b may be a key interacting partner for Sybu in germ plasm aggregation, mediating both local and FMA-mediated aggregation. Given the prominent role of Kif5b in multiple transport events in the egg and early embryo, it is likely that this motor is also involved in germ plasm aggregation at some level, although in general is little understood how the action of different kinesins and other motors is integrated and regulated for different transport substrates.

Sybu has been implicated in the kinesin-based anterograde transport of mitochondria in neurons (Su et al., 2004). Other adaptor proteins involved in anterograde or other aspects of mitochondrial transport include Milton/Oip106/Trak1, Rhot1/Miro, and RanBP2, primarily identified from studies in cultured neurons or in Drosophila (Frederick and Shaw, 2007). A recent study in Xenopus using a dominant-inhibitory construct implicated Rhot1/Miro in germ plasm aggregation, displaying results strikingly similar to Sybu depletion (Tada et al., 2016). Thus, germ plasm aggregation is likely to entail complex interactions between multiple kinesins and adaptor proteins, with unique and overlapping functions, and dynamic interaction with an also dynamic cytoskeleton.

In general, the mechanisms controlling the localization of organelles and supra-organellar structures such as germ plasm are little understood. Our works lends some insight into this process, showing that localization of mitochondria by Sybu-Kinesin complexes is likely important for different aspects of mitochondrial dynamics in dividing cells and gastrulae. Interestingly, Sybu is also thought to mediate the transport of so-called "dorsal determinants" in Xenopus and zebrafish. Our studies and those in fish show there is some variability in this requirement, which could suggest that Sybu is not the only adaptor protein involved. Also, since Sybu inhibition is achieved by acute depletion in Xenopus oocytes and by maternal genetic mutation in zebrafish, this comparison may not be exactly commensurable. There could also be a further requirement for Sybu-mediated localization during oocyte development. Indeed, rescue of the *tkk* dorsal axis mutant phenotype requires expression of a *sybu* transgene during oogenesis (Nojima et al., 2010). Additionally, the nature of *sybu* expression during early development and the fertility of maternal-zygotic *tkk* mutant fish would seem to rule out a role for Sybu in germ plasm aggregation and PGC specification in fish. Indeed, *sybu* RNA and protein are no longer detectable when germ plasm is transported and re-assembled at distal cleavage furrows in the zebrafish zygote.

This idea fits with the proposed model for germ plasm evolution, which suggests that maternally-localized germ plasm evolved independently in different animal lineages (Extavour and Akam, 2003) and germ plasm aggregation proceeds quite differently in zebrafish and in Xenopus. It is also interesting to note that another maternal mutation implicated in zebrafish dorsal axis formation, *hecate/grip2a*, is also apparently dispensable for PGC development, whereas its Xenopus homolog is involved in germ plasm function and likely dispensable for axis formation (Kirilenko et al., 2008; Ge et al., 2014). It may be that the functions of Sybu and Grip2a related to the germ plasm were lost concomitant with evolution of meroblastic cleavage (i.e., loss of cleavage at the vegetal pole) and preferentially retained transport of axis signaling components, whereas the converse may have predominated in Xenopus.

4. Materials and methods

4.1. Plasmids

The coding region of *sybu* (*sybu*.S) was amplified from a full-length cDNA obtained commercially (GenBank Accession: BC079762; GE/Dharmacon) and cloned into the pCR8/GW/TOPO vector (Invitrogen). Sequence verified clones were recombined into custom pCS2+ Gateway vectors for untagged and for C-terminal HA- and GFP-tagged versions (custom vector conversion kit; Invitrogen). *sybu-pCS2+* and tagged derivatives were linearized with *Not*I and capped mRNA was synthesized using a SP6 mMessage mMachine kit (Ambion).

4.2. Antisense oligos and host transfer

Antisense oligodeoxynucleotides (oligos) are phosphorothioate-phosphodiester chimeric oligos obtained from Integrated DNA Technologies (Coralville, Iowa) (* represent phosphorothioate bonds): *sybu234*, 5'-A*A*G*GAGATTCCGAAG*A*C*G-3' (new); *sybu_as6*, 5'-G*C*TACTGGCAGATGA*A*A*C-3' (Colozza and de Robertis, 2014); *kif3b*, G*A*G*CTCTTAGACTTGGA*C*A*T (new); *kif4a*, A*T*G*CCCTCATCCTTCCC*C*A*T (Robb et al., 1996).

Stage VI oocytes were manually defolliculated and injected with the appropriate *sybu* antisense oligos at the vegetal pole. After culturing for 24 h at 18 °C in oocyte culture medium [OCM; 70% Leibovitz L-15, 0.045% polyvinyl alcohol, 1x penicillin-streptomycin, pH7.6–7.8]

(modified from Heasman et al., 1991) oocytes were matured in 2 μM Progesterone. Rescue injections with 5 pg *sybu* mRNA were done right before oocyte maturation. Host transfer was carried out as described by Olson et al. (2012).

4.3. RT-PCR

Total RNA was isolated from flash frozen matured oocytes homogenized in cell lysis buffer (50 mM Tris pH7.5, 50 mM NaCl, 5 mM EDTA, 0.5% SDS, 250 mg/mL Proteinase K) incubated at 37 °C for 1 h. The mixture was further supplemented with 0.2 volumes 5 M ammonium acetate and 20 μg glycogen, extracted with phenol/chloroform/isoamyl alcohol and precipitated with 100% isopropanol. RNA was resuspended in nuclease free water, and treated with DNase I (10U; Roche Applied Science) for 30 min at 37 °C and precipitated with lithium chloride at −20 °C. Resuspended RNAs were primed with random hexamer primers and cDNA was generated with M-MLV reverse transcriptase (Invitrogen) for 30 min at 37 °C.

Levels of gene expression were quantified using real time PCR with the LightCycler480 System (Roche Applied Sciences) using either SYBR Green I Master Mix and/or Universal Probe Library hydrolysis probes as previously described (Houston and Wylie, 2005; Schneider et al., 2011). All samples were normalized to *ornithine decarboxylase* (*odc*) and levels of expression were calculated against a standard curve of diluted uninjected oocyte cDNA. Individual primers, probes, and PCR conditions are available upon request.

4.4. Whole mount in-situ hybridization

Whole mount in-situ hybridization was performed as previously described (Sive et al., 2000; Kerr et al., 2008). The *xpat/pgat* template was linearized with *Eco*RI and transcribed with T7 polymerase (Promega) to synthesize the antisense probe with digoxygenin-11-UTPs (Roche). s*ybu/pCMV-SPORT6*.1 was linearized with *Sma*I and transcribed with T7.

4.5. Germ plasm aggregation

For in vitro assays, oocytes were chemically defolliculated with collagenase and cultured overnight in OCM prior to injections of 6 ng *sybu234* or *sybu_as6* oligos at the vegetal pole. Oocytes were then incubated for 24 h and subsequently matured with 2 μM Progesterone for 20 h at 18 °C. Germ plasm islands were stained in 100 nM MitoTracker™ (ThermoFisher) for 15 min at room temperature and washed several times over 30 min in OCM. Oocytes were prick-activated in the animal pole, mimicking fertilization, and germ plasm aggregation was monitored by epifluorescence over 3 h. For in vivo assays, manually defolliculated oocytes were fertilized by the host-transfer procedure. Resulting embryos were dejellyed with 2% L-cysteine (Sigma) about 1 h post fertilization and stained with DiOC6(3) (1:1000, ThermoFisher) for 10 min, with gentle rocking. Embryos were washed several times in 0.1X MMR before the first cell division and imaged, starting about 80 min post-fertilization.

4.6. Microscopy and time lapse imaging

Microscopy was performed at room temperature on an inverted, wide-field epifluorescence microscope (DMI4000B, Leica) using a 5x objective. Images were acquired using a monochrome digital camera (DFC3000G camera, Leica) and Leica AF6000 (64 bit) software. The pixel size was 1.07 × 1.07 × 0.200 μm and image size was 512 × 512 pixels. Time lapse images were collected at twenty-second intervals. Exposure times were approximately 0.30 s on the FITC channel. Samples were kept in either OCM or 0.1x MMR solution for imaging. Embryos were placed in custom aluminum chamber slides cut to the size of a standard microscope slide. Cover slips were attached to the bottom of the wells (1 cm diameter) with nail polish. Images were taken at or near the vegetal pole. Activated oocytes were placed into a mesh grid and imaged through the mesh in serial fashion.

4.7. Image processing and quantitation

Movies were initially processed in Fiji/ImageJ v1.51n (64-bit). Images were cropped to the relevant germ plasm regions, adjusted for threshold manually and exported for analysis. Montage construction and kymograph analysis were performed in ImageJ using the respective plugins. Germ plasm area measurements were made manually in Fiji/ImageJ or using a custom script in MATLAB_R2015a (available on request). Parameters were statistically analyzed using one-way ANOVA or Kruskal-Wallis tests with appropriate post-hoc tests using MATLAB. Images were prepared for publication in Fiji/ImageJ and Adobe Photoshop/Illustrator; only minor level and contrast adjustments were made and applied uniformly to the entire image. Other modifications included resizing and changes to stroke/fill weights and colors and the addition of annotation overlays.

Acknowledgements

The authors would like to thank members of the Houston lab for discussions and for critical reading of the manuscript. This work was supported by NIH R01 GM083999 to DWH. DO received support through a graduate fellowship from the Developmental Studies Hybridoma Bank (DSHB).

Online supplementary material

Fig. S1 shows in situ hybridization of *sybu* during oogenesis and embryonic development (related to Fig. 1). **Videos 1 and 2** show representative time-lapse imaging movies of germ plasm aggregation in control and *sybu*-depleted host-transferred embryos, respectively (related to Figs. 6–7). **Video 3** is a movie of germ plasm aggregation in a *sybu* rescued embryo (related to Figs. 6–7). **Video 4** is a movie of a kif3b-depleted host-transferred embryo (related to Fig. 8). **Fig. S2** shows RT-PCR analysis of *kif3b* and *kif4a* mRNA levels in antisense oligo injected oocytes and *kif3b*-depleted gastrulae (related to Fig. 8). **Fig. S3** shows a montage of frames from Video 4 and a kymograph analysis of mitochondrial movement from that sample (related to Fig. 8, Video 4).

Supplementary material related to this article can be found online at doi:10.1016/j.ydbio.2017.10.006.

Appendix A. Supporting information

Supplementary data associated with this article can be found in the online version at doi:10.1016/j.ydbio.2017.10.006.

References

Aguero, T., Kassmer, S., Alberio, R., Johnson, A., King, M.L., 2017. Mechanisms of vertebrate germ cell determination. In: Vertebrate Development. Springer, pp. 383–440.

Beams, H.W., Kessel, R.G., 1974. The problem of germ cell determinants. Int. Rev. Cytol. 39, 413–479.

Betley, J.N., Heinrich, B., Vernos, I., Sardet, C., Prodon, F., Deshler, J.O., 2004. Kinesin II mediates Vg1 mRNA transport in Xenopus oocytes. Curr. Biol. 14, 219–224. http://dx.doi.org/10.1016/j.cub.2004.01.028.

Cai, Q., Gerwin, C., Sheng, Z.-H., 2005. Syntabulin-mediated anterograde transport of mitochondria along neuronal processes. J. Cell Biol. 170, 959–969. http://dx.doi.org/10.1083/jcb.200506042.

Cai, Q., Pan, P.-Y., Sheng, Z.-H., 2007. Syntabulin-kinesin-1 family member 5B-mediated axonal transport contributes to activity-dependent presynaptic assembly. J. Neurosci. 27, 7284–7296. http://dx.doi.org/10.1523/JNEUROSCI.0731-07.2007.

Chan, A.P., Kloc, M., Larabell, C.A., LeGros, M., Etkin, L.D., 2007. The maternally localized RNA fatvg is required for cortical rotation and germ cell formation. Mech. Dev. 124, 350–363. http://dx.doi.org/10.1016/j.mod.2007.02.001.

Choo, S., Heinrich, B., Betley, J.N., Chen, Z., Deshler, J.O., 2005. Evidence for common

machinery utilized by the early and late RNA localization pathways in Xenopus oocytes. Dev. Biol. 278, 103–117. http://dx.doi.org/10.1016/j.ydbio.2004.10.019.
Colozza, G., De Robertis, E.M., 2014. Maternal syntabulin is required for dorsal axis formation and is a germ plasm component in Xenopus. Differentiation. http://dx.doi.org/10.1016/j.diff.2014.03.002.
Cuykendall, T.N., Houston, D.W., 2009. Vegetally localized Xenopus trim36 regulates cortical rotation and dorsal axis formation. Development 136 (3057–3065). http://dx.doi.org/10.1242/dev.036855.
Czołowska, R., 1969. Observations on the origin of the "germinal cytoplasm" in *Xenopus laevis*. J. Embryol. Exp. Morphol. 22, 229–251. http://dx.doi.org/10.1007/BF00580253.
Danilchik, M.V., Bedrick, S.D., Brown, E.E., Ray, K., 2003. Furrow microtubules and localized exocytosis in cleaving *Xenopus laevis* embryos. J. Cell Sci. 116, 273–283.
Eddy, E., 1975. Germ plasm and the differentiation of the germ cell line. Int Rev. Cytol. 43, 229–280.
Eno, C., Pelegri, F., 2016. Germ Cell Determinant Transmission, Segregation, and Function in the Zebrafish Embryo. InTech. http://dx.doi.org/10.5772/62207.
Extavour, C.G., Akam, M., 2003. Mechanisms of germ cell specification across the metazoans: epigenesis and preformation. Development 130, 5869–5884. http://dx.doi.org/10.1242/dev.00804.
Frederick, R.L., Shaw, J.M., 2007. Moving mitochondria: establishing distribution of an essential organelle. Traffic 8, 1668–1675. http://dx.doi.org/10.1111/j.1600-0854.2007.00644.x.
Ge, X., Grotjahn, D., Welch, E., Lyman Gingerich, J., Holguin, C., Dimitrova, E., Abrams, E.W., Gupta, T., Marlow, F.L., Yabe, T., Adler, A., Mullins, M.C., Pelegri, F., 2014. Hecate/Grip2a acts to reorganize the cytoskeleton in the symmetry-breaking event of embryonic axis induction. PLoS Genet. 10, e1004422. http://dx.doi.org/10.1371/journal.pgen.1004422.
Heasman, J., Holwill, S., Wylie, C.C., 1991. Fertilization of cultured Xenopus oocytes and use in studies of maternally inherited molecules. Methods Mol. Biol. 36, 213–230.
Hellsten, U., Harland, R.M., Gilchrist, M.J., Hendrix, D., Jurka, J., Kapitonov, V., Ovcharenko, I., Putnam, N.H., Shu, S., Taher, L., Blitz, I.L., Blumberg, B., Dichmann, D.S., Dubchak, I., Amaya, E., Detter, J.C., Fletcher, R., Gerhard, D.S., Goodstein, D., Graves, T., Grigoriev, I.V., Grimwood, J., Kawashima, T., Lindquist, E., Lucas, S.M., Mead, P.E., Mitros, T., Ogino, H., Ohta, Y., Poliakov, A.V., Pollet, N., Robert, J., Salamov, A., Sater, A.K., Schmutz, J., Terry, A., Vize, P.D., Warren, W.C., Wells, D., Wills, A., Wilson, R.K., Zimmerman, L.B., Zorn, A.M., Grainger, R., Grammer, T., Khokha, M.K., Richardson, P.M., Rokhsar, D.S., 2010. The genome of the Western clawed frog Xenopus tropicalis. Science 328, 633–636. http://dx.doi.org/10.1126/science.1183670.
Hirokawa, N., Noda, Y., Tanaka, Y., Niwa, S., 2009. Kinesin superfamily motor proteins and intracellular transport. Nat. Rev. Mol. Cell Biol. 10, 682–696. http://dx.doi.org/10.1038/nrm2774.
Houston, D.W., King, M.L., 2000. Germ plasm and molecular determinants of germ cell fate. Curr. Top. Dev. Biol. 50, 155–181.
Houston, D.W., Wylie, C.C., 2005. Maternal Xenopus Zic2 negatively regulates Nodal-related gene expression during anteroposterior patterning. Development 132, 4845–4855. http://dx.doi.org/10.1242/dev.02066.
Houston, D.W., 2013. Regulation of cell polarity and RNA localization in vertebrate oocytes. Int. Rev. Cell Mol. Biol. 306, 127–185. http://dx.doi.org/10.1016/B978-0-12-407694-5.00004-3.
Houston, D.W., 2017. Vertebrate axial patterning: from egg to asymmetry. Adv. Exp. Med. Biol. 953, 209–306. http://dx.doi.org/10.1007/978-3-319-46095-6_6.
Hudson, C., Woodland, H.R., 1998. Xpat, a gene expressed specifically in germ plasm and primordial germ cells of Xenopus laevis. Mech. Dev. 73, 159–168.
Hulstrand, A.M., Schneider, P.N., Houston, D.W., 2010. The use of antisense oligonucleotides in Xenopus oocytes. Methods 51, 75–81. http://dx.doi.org/10.1016/j.ymeth.2009.12.015.
James-Zorn, C., Ponferrada, V.G., Burns, K.A., Fortriede, J.D., Lotay, V.S., Liu, Y., Brad Karpinka, J., Karimi, K., Zorn, A.M., Vize, P.D., 2015. Xenbase: core features, data acquisition, and data processing. Genesis 53, 486–497. http://dx.doi.org/10.1002/dvg.22873.
Kaneshiro, K., Miyauchi, M., Tanigawa, Y., Ikenishi, K., Komiya, T., 2007. The mRNA coding for Xenopus glutamate receptor interacting protein 2 (XGRIP2) is maternally transcribed, transported through the late pathway and localized to the germ plasm. Biochem. Biophys. Res. Commun. 355, 902–906. http://dx.doi.org/10.1016/j.bbrc.2007.02.059.
Karpinka, J.B., Fortriede, J.D., Burns, K.A., James-Zorn, C., Ponferrada, V.G., Lee, J., Karimi, K., Zorn, A.M., Vize, P.D., 2015. Xenbase, the Xenopus model organism database; new virtualized system, data types and genomes. Nucleic Acids Res. 43, D756–D763. http://dx.doi.org/10.1093/nar/gku956.
Kerr, T.C., Cuykendall, T.N., Luettjohann, L.C., Houston, D.W., 2008. Maternal Tgif1 regulates nodal gene expression in Xenopus. Dev. Dyn. 237, 2862–2873. http://dx.doi.org/10.1002/dvdy.21707.
Kirilenko, P., Weierud, F.K., Zorn, A.M., Woodland, H.R., 2008. The efficiency of Xenopus primordial germ cell migration depends on the germplasm mRNA encoding the PDZ domain protein Grip2. Differentiation 76, 392–403. http://dx.doi.org/10.1111/j.1432-0436.2007.00229.x.
Kloc, M., Dougherty, M.T., Bilinski, S., Chan, A.P., Brey, E., King, M.L., Patrick, C.W., Etkin, L.D., 2002. Three-dimensional ultrastructural analysis of RNA distribution within germinal granules of Xenopus. Dev. Biol. 241, 79–93. http://dx.doi.org/10.1006/dbio.2001.0488.
Kloc, M., Etkin, L.D., 1995. Two distinct pathways for the localization of RNAs at the vegetal cortex in Xenopus oocytes. Development 121, 287–297.
Kloc, M., Larabell, C., Chan, A.P., Etkin, L.D., 1998. Contribution of METRO pathway localized molecules to the organization of the germ cell lineage. Mech. Dev. 75, 81–93.
Mei, W., Jin, Z., Lai, F., Schwend, T., Houston, D.W., King, M.L., Yang, J., 2013. Maternal Dead-End1 is required for vegetal cortical microtubule assembly during Xenopus axis specification. Development 140, 2334–2344. http://dx.doi.org/10.1242/dev.094748.
Messitt, T.J., Gagnon, J.A., Kreiling, J.A., Pratt, C.A., Yoon, Y.J., Mowry, K.L., 2008. Multiple kinesin motors coordinate cytoplasmic RNA transport on a subpopulation of microtubules in Xenopus oocytes. Dev. Cell 15, 426–436. http://dx.doi.org/10.1016/j.devcel.2008.06.014.
Nojima, H., Rothhamel, S., Shimizu, T., Kim, C.H., Yonemura, S., Marlow, F.L., Hibi, M., 2010. Syntabulin, a motor protein linker, controls dorsal determination. Development 137, 923–933. http://dx.doi.org/10.1242/dev.046425.
Olson, D.J., Hulstrand, A.M., Houston, D.W., 2012. Maternal mRNA knock-down studies: antisense experiments using the host-transfer technique in Xenopus laevis and Xenopus tropicalis. Methods Mol. Biol. 917, 167–182. http://dx.doi.org/10.1007/978-1-61779-992-1_10.
Quaas, J., Wylie, C.C., 2002. Surface contraction waves (SCWs) in the Xenopus egg are required for the localization of the germ plasm and are dependent upon maternal stores of the kinesin-like protein Xklp1. Dev. Biol. 243, 272–280. http://dx.doi.org/10.1006/dbio.2001.0564.
Ressom, R., Dixon, K., 1988. Relocation and reorganization of germ plasm in Xenopus embryos after fertilization. Development 103, 507–518.
Savage, R.M., Danilchik, M.V., 1993. Dynamics of germ plasm localization and its inhibition by ultraviolet irradiation in early cleavage Xenopus embryos. Dev. Biol. 157, 371–382. http://dx.doi.org/10.1006/dbio.1993.1142.
Robb, D.L., Heasman, J., Raats, J., Wylie, C.C., 1996. A kinesin-like protein is required for germ plasm aggregation in Xenopus. Cell 87, 823–831.
Schneider, P.N., Olthoff, J.T., Matthews, A.J., Houston, D.W., 2011. Use of fully modified 2'-O-methyl antisense oligos for loss-of-function studies in vertebrate embryos. Genesis 49, 117–123. http://dx.doi.org/10.1002/dvg.20689.
Session, A.M., Uno, Y., Kwon, T., Chapman, J.A., Toyoda, A., Takahashi, S., Fukui, A., Hikosaka, A., Suzuki, A., Kondo, M., van Heeringen, S.J., Quigley, I., Heinz, S., Ogino, H., Ochi, H., Hellsten, U., Lyons, J.B., Simakov, O., Putnam, N., Stites, J., Kuroki, Y., Tanaka, T., Michiue, T., Watanabe, M., Bogdanovic, O., Lister, R., Georgiou, G., Paranjpe, S.S., van Kruijsbergen, I., Shu, S., Carlson, J., Kinoshita, T., Ohta, Y., Mawaribuchi, S., Jenkins, J., Grimwood, J., Schmutz, J., Mitros, T., Mozaffari, S.V., Suzuki, Y., Haramoto, Y., Yamamoto, T.S., Takagi, C., Heald, R., Miller, K., Haudenschild, C., Kitzman, J., Nakayama, T., Izutsu, Y., Robert, J., Fortriede, J., Burns, K., Lotay, V., Karimi, K., Yasuoka, Y., Dichmann, D.S., Flajnik, M.F., Houston, D.W., Shendure, J., DuPasquier, L., Vize, P.D., Zorn, A.M., Ito, M., Marcotte, E.M., Wallingford, J.B., Ito, Y., Asashima, M., Ueno, N., Matsuda, Y., Veenstra, G.J.C., Fujiyama, A., Harland, R.M., Taira, M., Rokhsar, D.S., 2016. Genome evolution in the allotetraploid frog Xenopus laevis. Nature 538, 336–343. http://dx.doi.org/10.1038/nature19840.
Shindo, A., Yamamoto, T.S., Ueno, N., 2008. Coordination of cell polarity during Xenopus gastrulation. PLoS One 3, e1600. http://dx.doi.org/10.1371/journal.pone.0001600.
Sive, H., Grainger, R., Harland, R., 2000. Early Development of *Xenopus laevis*: A Laboratory Manual. CSHL Press, Cold Spring Harbor NY.
Su, Q., Cai, Q., Gerwin, C., Smith, C.L., Sheng, Z.-H., 2004. Syntabulin is a microtubule-associated protein implicated in syntaxin transport in neurons. Nat. Cell Biol. 6, 941–953. http://dx.doi.org/10.1038/ncb1169.
Tada, H., Taira, Y., Morichika, K., Kinoshita, T., 2016. Mitochondrial trafficking through Rhot1 is involved in the aggregation of germinal granule components during primordial germ cell formation in Xenopus embryos. Dev. Growth Differ. 58, 641–650. http://dx.doi.org/10.1111/dgd.12310.
Tarbashevich, K., Koebernick, K., Pieler, T., 2007. XGRIP2.1 is encoded by a vegetally localizing, maternal mRNA and functions in germ cell development and anteroposterior PGC positioning in Xenopus laevis. Dev. Biol. 311, 554–565. http://dx.doi.org/10.1016/j.ydbio.2007.09.012.
Theusch, E.V., Brown, K.J., Pelegri, F., 2006. Separate pathways of RNA recruitment lead to the compartmentalization of the zebrafish germ plasm. Dev. Biol. 292, 129–141. http://dx.doi.org/10.1016/j.ydbio.2005.12.045.
Venkatarama, T., Lai, F., Luo, X., Zhou, Y., Newman, K., King, M.L., 2010. Repression of zygotic gene expression in the Xenopus germline. Development 137, 651–660. http://dx.doi.org/10.1242/dev.038554.
Voronina, E., Seydoux, G., Sassone-Corsi, P., Nagamori, I., 2011. RNA granules in germ cells. Cold Spring Harb. Perspect. Biol., 3. http://dx.doi.org/10.1101/cshperspect.a002774.
Whitington, P., Dixon, K., 1975. Quantitative studies of germ plasm and germ cells during early embryogenesis of Xenopus laevis. J. Embryol. Exp. Morphol. 33, 57–74.
Willemsen, M.H., Ba, W., Wissink-Lindhout, W.M., de Brouwer, A.P.M., Haas, S.A., Bienek, M., Hu, H., Vissers, L.E.L.M., van Bokhoven, H., Kalscheuer, V., Nadif Kasri, N., Kleefstra, T., 2014. Involvement of the kinesin family members KIF4Aand KIF5Cin intellectual disability and synaptic function. J. Med. Genet. 51, 487–494. http://dx.doi.org/10.1136/jmedgenet-2013-102182.